arXiv:1611.02809v1 [physics.soc-ph] 9 Nov 2016

Sudden spreading of infections in an epidemic model with a finite seed fraction

Takehisa Hasegawa[1,*] and Koji Nemoto[2,†]

[1] *Department of Mathematics and Informatics, Ibaraki University, 2-1-1, Bunkyo, Mito, 310-8512, Japan*
[2] *Department of Physics, Hokkaido University, Kita 10 Nishi 8, Kita-ku, Sapporo, Hokkaido, 060-0810, Japan*

We study a simple case of the susceptible-weakened-infected-removed model in regular random graphs in a situation where an epidemic starts from a finite fraction of initially infected nodes (seeds). Previous studies have shown that, assuming a single seed, this model exhibits a kind of discontinuous transition at a certain value of infection rate. Performing Monte Carlo simulations and evaluating approximate master equations, we find that the present model has two critical infection rates with a finite seed fraction. At the first critical rate the system shows a percolation transition of clusters composed of removed nodes, and at the second critical rate, which is larger than the first one, a giant cluster suddenly grows and the order parameter jumps even though it has been already rising. Numerical evaluation of the master equations shows that such sudden epidemic spreading does occur if the degree of the underlying network is large and the seed fraction is small.

PACS numbers: 89.75.Hc,87.23.Ge,05.70.Fh,64.60.aq

I. INTRODUCTION

Contagion processes such as infectious diseases, opinion formations, and information propagations, are ubiquitous in our networked society. Network science has shown the profound impact that network structures give on such spreading behaviors [1–4]. An epidemic can spread globally and infect a large number of individuals even if its infection rate is infinitesimally small, when the underlying network is highly heterogeneous [5, 6]; such events can be described by simple infectious disease models, such as the susceptible-infected-removed (SIR) model [7] and the susceptible-infected-susceptible model [8]. Extensive studies [9] on simple epidemic models in complex networks have developed accurate approximations with which the time evolution of epidemic spreading is well described [10–13], and they have discovered new phenomena owing to the complex structure of the networks, such as the localization of epidemics [14, 15] and the stretching of criticality [16–18]. Alongside these studies, a similar amount of effort has been devoted to contagion processes in social dynamics in order to recognize the effect of network connecting individuals on human behaviors, such as opinion formations and the propagation processes of information, innovations, and transient fads [19].

Social reinforcement, which means that an individual requires multiple prompts from neighbors before adopting information, has received attention in recent years. Centola confirmed the effect of social reinforcement in individuals' behavior through experiments on online social networks [20, 21]. After this, several social contagion models incorporating social reinforcement have been proposed [22–30]. Krapivsky et al. [22] put forward a mathematical model for transient fads, which we call the fad model. The fad model is a variant of the SIR model, in which intermediate states are added between the S and I states (corresponding to uninformed and adopter in the fad context, respectively). This model was analyzed by the rate equation which assumes a well-mixed population (i.e., the mean-field approximation) and it showed that its transition is explosive in the sense that, at a certain value of infection rate, the number of individuals that adopted information suddenly grows and the order parameter discontinuously jumps from zero to a non-zero value. We previously studied a discrete-time fad model in uncorrelated networks in order to confirm that discontinuous transition occurs when the network is not highly heterogeneous [26]. Similar discontinuous transitions have been reported in generalized epidemic models [31–35]. Very recently, the susceptible-weakened-infected-removed (SWIR) model, which is a variation of the SIR model with an additional "weakened" state, has been studied [34, 35]. Branching process analysis and numerical simulations have demonstrated that, in random graphs, a single infected node in this model can trigger an infinite avalanche of macroscopic order; this indicates the existence of a discontinuous transition within appropriate model parameters.

In this paper, we study the SWIR model placed in a network, but assume that an epidemic starts from a finite fraction of initially infected nodes (seeds). Few studies have investigated the effect of initial conditions on SIR-type epidemic models [36–38], although we have previously studied the SIR model with a finite seed fraction in order to

*Electronic address: takehisa.hasegawa.sci@vc.ibaraki.ac.jp
†Electronic address: nemoto@statphys.sci.hokudai.ac.jp

show that the critical infection rate, above which there is a giant cluster of R nodes in a network, crucially depends on the seed fraction ρ [39]. When this fraction is finite ($\rho > 0$), each seed creates a cluster of R nodes and these clusters sometimes form a giant cluster by connecting with each other; individuals seeds, however, do not have the potential to induce a global outbreak all by themselves. The critical infection rate of this SIR model is, therefore, smaller than the so-called epidemic threshold. At rate above this threshold, a single seed can spread through the network; but as long as $\rho > 0$, it does not exhibit any singularities at the threshold. The aim of this paper is to observe what happens when ρ for the SWIR model is finite. We perform Monte Carlo simulations for the SWIR model in a regular random graph (RRG) so as to show that the discontinuity of the order parameter holds for the present case, and that the model also exhibits an ordinary percolation transition at a smaller rate. We also investigate the SWIR model using approximate master equations (AMEs) [11–13, 39] in order to find that a discontinuous transition occurs if the degree of the underlying network is large and the seed fraction is small.

II. MODEL

Let us consider the SWIR model in a static network with N nodes. Each node in the network takes one of the following four states: susceptible (S), weakened (W), infected (I), or removed (R). As an initial state of each trial, a fraction, ρ, of nodes is randomly chosen as seeds and is initially I, while other nodes are S. The system evolves as

$$\begin{aligned}
&\mathrm{S} + \mathrm{I} \to \mathrm{I} + \mathrm{I} \quad \text{with infection rate } \kappa,\\
&\mathrm{S} + \mathrm{I} \to \mathrm{W} + \mathrm{I} \quad \text{with infection rate } \lambda_1,\\
&\mathrm{W} + \mathrm{I} \to \mathrm{I} + \mathrm{I} \quad \text{with infection rate } \lambda_2,\\
&\mathrm{I} \to \mathrm{R} \quad \text{with removal rate } \mu.
\end{aligned}$$

Dynamics stop when I nodes no longer exist in the network. In other words, when only S, W, and R nodes remain.

The case where $\lambda_1 = \lambda_2 = 0$ corresponds to an ordinary SIR model, whose transition is a continuous one. The SWIR model shows a discontinuous transition when two additional processes ($\mathrm{S} + \mathrm{I} \to \mathrm{W} + \mathrm{I}$ and $\mathrm{W} + \mathrm{I} \to \mathrm{I} + \mathrm{I}$) work effectively. Lee et al. [34] studied the time evolution of a giant cluster in an SWIR model in order to determine the mechanism causing explosive spreading to occur from a single seed. Choi et al. [35] investigated an SWIR model with a single seed and $\kappa = 0$, $\lambda_1 = \lambda$, and $\lambda_2 = \mu = 1$ in random graphs and found that the transition is rather mixed order; what is meant by this is that an order parameter exhibits a discontinuous jump without any critical behavior while other physical quantities exhibit critical behaviors when the average degree is large. In our study, we consider an SWIR model with $\kappa = 0$ and $\lambda_1 = \lambda_2 = \lambda$, which corresponds to the fad model containing one intermediate state. When an S or W node is adjacent to an I node, this node becomes W or I, respectively, with probability $\lambda\Delta t$ within a short time Δt. This probability is independently given by each of the I nodes, and so the total infection rate at an S or W node is proportional to the number of I neighbors. An I node becomes R at a rate μ irrespective of the neighbors' states. Without loss of generality, we set $\mu = 1$ unless otherwise specified.

In the rest of this section, we briefly review the SIR model in an RRG in order to introduce the order parameter responsible for the characterization of the phase transition. When there is a single seed, or the fraction of infected seeds is infinitesimally small ($\rho \to 0$), the SIR model undergoes a phase transition at the epidemic threshold, $\kappa_c(\rho \to 0)$. Let us consider the mean fraction of the outbreak size (the number of R nodes), $\langle r \rangle$, where $\langle \cdot \rangle$ represents the average taken over all trials. In the limit $N \to \infty$, the system has two phases: (i) the local epidemic phase where $\langle r \rangle = 0$ for $\kappa < \kappa_c(\rho \to 0)$ and (ii) the global epidemic phase where $\langle r \rangle > 0$ for $\kappa > \kappa_c(\rho \to 0)$. Around κ_c, the SIR model exhibits typical critical behaviors with the same universality class as (dynamic) percolation [40, 41]. When the dynamics start from a finite fraction of I nodes, $\rho > 0$, the phase transition can be described in terms of percolation [42]. Connected components of R nodes are hereafter called R clusters. In the case of $\rho > 0$, a final state will contain numerous R clusters. The order parameter can then be given as $\langle r_{\max} \rangle = \langle R_{\max} \rangle / N$, where $\langle R_{\max} \rangle$ is the mean size of the largest R cluster. The SIR model has a critical infection rate $\kappa_c(\rho)$ such that $\langle r_{\max} \rangle$ decreases to zero as N increases for $\kappa < \kappa_c(\rho)$ and converges to a nonzero value with increasing N for $\kappa > \kappa_c(\rho)$. The phase transition at $\kappa_c(\rho)$ can be described in terms of percolation and its critical exponents are the same as those of percolation in the same network [39]. The critical infection rate $\kappa_c(\rho)$ depends on the seed fraction ρ, and deviates rapidly from the epidemic threshold $\kappa_c(\rho \to 0)$ as $\kappa_c(\rho \to 0) - \kappa_c(\rho) \sim \rho^{1/3}$ [39]. Note that $\langle r \rangle$ is not appropriate to describe the (continuous) transition for $\rho > 0$ because $\langle r \rangle > \rho > 0$, while, in the single seed case, R cluster is always unique and thus $\langle r \rangle = \langle r_{\max} \rangle$.

In the following section, we study an SWIR model with $\kappa = 0$ and $\lambda_1 = \lambda_2 = \lambda$. As is expected from the mean-field dynamics [22], it shows a discontinuous transition when the underlying network is homogeneous. In order to investigate dynamics in some details, we focus on the RRG where all the nodes have the same degree z.

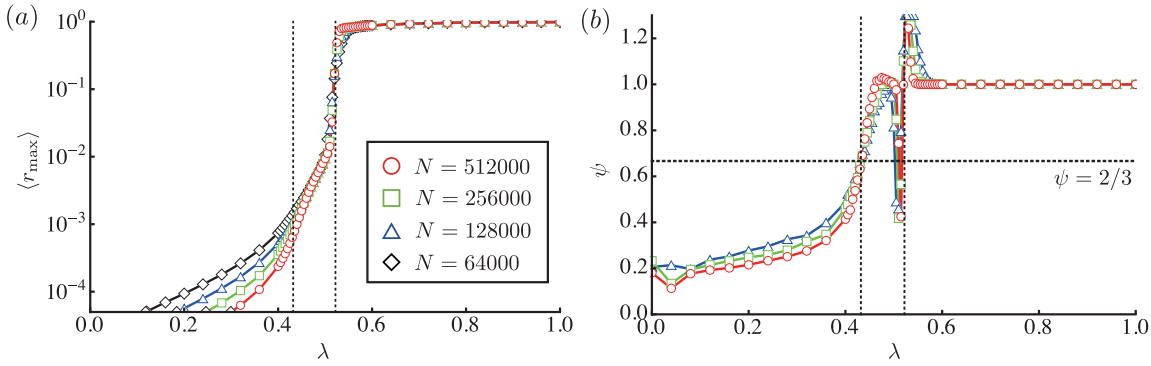

FIG. 1: Numerical results of (a) the order parameter $\langle r_{\max}\rangle(N)$ and (b) the fractal exponent $\psi(N)$ for the SWIR model in the RRG with $z = 9$. The two dotted lines represent $\lambda_c \approx 0.432$ (left) and $\lambda_d \approx 0.522$ (right).

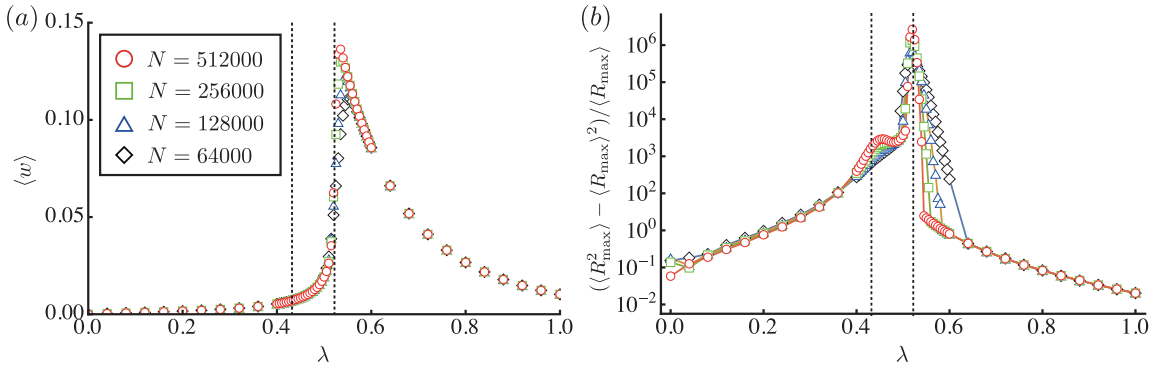

FIG. 2: (a) The mean fraction of W nodes $\langle w\rangle$ and (b) the sample-to-sample fluctuation of the largest cluster size, as a function of λ. The two dotted lines represent $\lambda_c \approx 0.432$ (left) and $\lambda_d \approx 0.522$ (right).

III. RESULTS

First, we perform Monte Carlo simulations for the SWIR model in the RRG with $z = 9$. The number of nodes is $N = 64000, 128000, 256000$, and 512000. The number of graph realizations is 100, and the number of trials on each graph is 500. Seeds are randomly chosen at each trial and the fraction of seeds is $\rho = 0.001$.

The order parameter $\langle r_{\max}\rangle$ is shown in Fig. 1 (a) for the RRGs of several sizes. The N-dependence of the order parameter indicates that there are two critical infection rates: λ_c, below which $\langle r_{\max}\rangle$ tends to zero as N increases and above which $\langle r_{\max}\rangle$ converges to a nonzero value; and λ_d, around which $\langle r_{\max}\rangle$ rises more sharply in larger networks and eventually shows a discontinuous jump in the limit $N \to \infty$.

In order to obtain the first critical rate, λ_c, numerically, we evaluate the fractal exponent, ψ $(0 \le \psi \le 1)$, of the largest R cluster, $\langle R_{\max}\rangle \propto N^{\psi}$ [43, 44]. The fractal exponent in finite networks, $\psi(N)$, is given and approximated by $\psi = \mathrm{d}\ln\langle R_{\max}\rangle(N)/\mathrm{d}\ln N \approx (\ln\langle R_{\max}\rangle(N) - \ln\langle R_{\max}\rangle(N/2))/(\ln N - \ln(N/2))$. As N increases, $\psi(N)$ goes to zero for $\lambda < \lambda_c$ and to one for $\lambda > \lambda_c$, thereby reflecting that $\langle R_{\max}\rangle \sim O(1)$ for $\lambda < \lambda_c$ and $\sim O(N)$ for $\lambda > \lambda_c$. As shown in Fig. 1 (b), $\psi(N)$ of several networks of different sizes crosses at a unique point, giving $\lambda_c \approx 0.432$. The transition at λ_c is of an ordinary percolation, $\psi \approx 2/3$ at $\lambda = \lambda_c$, and $\langle R_{\max}\rangle$ around λ_c obeys a finite size scaling [43] if $\langle r_{\max}\rangle(\lambda) - \langle r_{\max}\rangle(\lambda_c) \sim |\lambda - \lambda_c|^{\beta}$ with $\beta = 1$ is assumed (not shown). The values of ψ and β obtained here are also observed for the SIR model with $\rho > 0$ in the RRG [39]. An apparent oscillatory deviation from $\psi = 1$ is seen at $\lambda_d \approx 0.522$; however, this deviation is a finite size effect due to the occurrence of the discontinuous jump. Indeed, the width of the deviating region tends to shrink as the size increases.

The discontinuous jump of the order parameter at λ_d is due to the additional state W. As shown in Fig. 2 (a), the fraction of W nodes $\langle w\rangle$ shows characteristic behavior around λ_d: $\langle w\rangle$ increases with λ below λ_d, jumps to a peak value at λ_d, and then decreases above λ_d. A large number of W nodes are necessary for the strong activation of the $\mathrm{W} + \mathrm{I} \to \mathrm{I} + \mathrm{I}$ process to occur just before the explosive growth of R clusters, as has previously been mentioned for the case of single seed [34]. In the case of a finite seed fraction, such abundant W nodes are supplied more efficiently

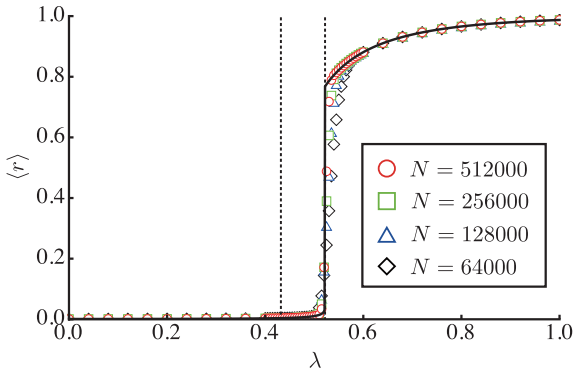

FIG. 3: The fraction of removed nodes, $\langle r\rangle$, as a function of λ for the SWIR model in the RRG with $z = 9$. The solid line is drawn from the AMEs, and the symbols represent Monte Carlo results. The two dotted lines represent $\lambda_c \approx 0.432$ (left) and $\lambda_d \approx 0.522$ (right).

because a number of W nodes peripheral to the finite R clusters are created by abundant seeds. Although the system already has a macroscopic order for $\lambda_c < \lambda$ (the largest R cluster size $\langle R_{\max}\rangle$ becomes $O(N)$), the system exhibits a characteristic behavior; this behavior is that the largest R cluster remains very small for $\lambda_c < \lambda < \lambda_d$ and before growing explosively at λ_d. The sample-to-sample fluctuation of the largest R cluster size, $(\langle R_{\max}^2\rangle - \langle R_{\max}\rangle^2)/\langle R_{\max}\rangle$, shows a higher peak at λ_d than at λ_c, although both peaks grow with N and eventually diverge when $N \gg 1$ (Fig. 2 (b)).

Next, we describe the SWIR model in an infinitely large RRG of $z \geq 2$ using the approximate master equations (AMEs) [11–13, 39]. Let $s_{\ell,m,n}(t)$, $w_{\ell,m,n}(t)$, $i_{\ell,m,n}(t)$, and $r_{\ell,m,n}(t)$ be the fractions of S, W, I, and R nodes, respectively, having ℓ susceptible, m weakened, and n infected neighbors (the remaining $\tilde{z} = z - \ell - m - n$ neighbors are removed) at time t. The conservation law, $s_{\ell,m,n}(t) + w_{\ell,m,n}(t) + i_{\ell,m,n}(t) + r_{\ell,m,n}(t) = 1$, holds for any value of t. Note that S and W nodes change their states to W and I, respectively, with the rate λn if they have n infected neighbors.

Following [39] (see also [12, 13]), we obtain the master equation for the evolution of each density as

$$\begin{aligned}
\dot{s}_{\ell,m,n} =& -\lambda n s_{\ell,m,n} + \beta_{\rm S}^{\rm SW}[(\ell+1)s_{\ell+1,m-1,n} - \ell s_{\ell,m,n}] \\
&+ \beta_{\rm S}^{\rm WI}[(m+1)s_{\ell,m+1,n-1} - m s_{\ell,m,n}] + \mu[(n+1)s_{\ell,m,n+1} - n s_{\ell,m,n}], && \text{(1a)}\\
\dot{w}_{\ell,m,n} =& \lambda n s_{\ell,m,n} - \lambda n w_{\ell,m,n} + \beta_{\rm W}^{\rm SW}[(\ell+1)w_{\ell+1,m-1,n} - \ell w_{\ell,m,n}] \\
&+ \beta_{\rm W}^{\rm WI}[(m+1)w_{\ell,m+1,n-1} - m w_{\ell,m,n}] + \mu[(n+1)w_{\ell,m,n+1} - n w_{\ell,m,n}], && \text{(1b)}\\
\dot{i}_{\ell,m,n} =& \lambda n w_{\ell,m,n} - \mu i_{\ell,m,n} + \beta_{\rm I}^{\rm SW}[(\ell+1)i_{\ell+1,m-1,n} - \ell i_{\ell,m,n}] \\
&+ \beta_{\rm I}^{\rm WI}[(m+1)i_{\ell,m+1,n-1} - m i_{\ell,m,n}] + \mu[(n+1)i_{\ell,m,n+1} - n i_{\ell,m,n}], && \text{(1c)}\\
\dot{r}_{\ell,m,n} =& \mu i_{\ell,m,n} + \beta_{\rm R}^{\rm SW}[(\ell+1)r_{\ell+1,m-1,n} - \ell r_{\ell,m,n}] \\
&+ \beta_{\rm R}^{\rm WI}[(m+1)r_{\ell,m+1,n-1} - m r_{\ell,m,n}] + \mu[(n+1)r_{\ell,m,n+1} - n r_{\ell,m,n}]. && \text{(1d)}
\end{aligned}$$

In each of these equations, $\beta_{\rm X}^{\rm YZ}$ represents the rate at which a randomly chosen neighbor of a randomly chosen node in the state X (= S, W, I, R) changes its state from Y (= S, W) to Z (= W, I); this can be approximated as the rate at which an X-Y edge is changed to an X-Z edge [13], as shown in the below equations.

$$\beta_{\rm S}^{\rm SW} = \lambda\frac{\sum_{\ell,m,n}\ell n s_{\ell,m,n}}{\sum_{\ell,m,n}\ell s_{\ell,m,n}},\ \beta_{\rm W}^{\rm SW} = \lambda\frac{\sum_{\ell,m,n} m n s_{\ell,m,n}}{\sum_{\ell,m,n} m s_{\ell,m,n}},\ \beta_{\rm I}^{\rm SW} = \lambda\frac{\sum_{\ell,m,n} n^2 s_{\ell,m,n}}{\sum_{\ell,m,n} n s_{\ell,m,n}},\ \beta_{\rm R}^{\rm SW} = \lambda\frac{\sum_{\ell,m,n}\tilde{z} n s_{\ell,m,n}}{\sum_{\ell,m,n}\tilde{z} s_{\ell,m,n}}, \quad \text{(2a)}$$

$$\beta_{\rm S}^{\rm WI} = \lambda\frac{\sum_{\ell,m,n}\ell n w_{\ell,m,n}}{\sum_{\ell,m,n}\ell w_{\ell,m,n}},\ \beta_{\rm W}^{\rm WI} = \lambda\frac{\sum_{\ell,m,n} m n w_{\ell,m,n}}{\sum_{\ell,m,n} m w_{\ell,m,n}},\ \beta_{\rm I}^{\rm WI} = \lambda\frac{\sum_{\ell,m,n} n^2 w_{\ell,m,n}}{\sum_{\ell,m,n} n w_{\ell,m,n}},\ \beta_{\rm R}^{\rm WI} = \lambda\frac{\sum_{\ell,m,n}\tilde{z} n w_{\ell,m,n}}{\sum_{\ell,m,n}\tilde{z} w_{\ell,m,n}}. \quad \text{(2b)}$$

In these equations, the summations run over all $0 \leq \ell + m + n \leq z$. The initial state where a fraction $\rho(> 0)$ of nodes is randomly chosen as seeds is given by

$$s_{\ell,m,n}(0) = \delta_{z,\ell+n}(1-\rho)\binom{z}{\ell}(1-\rho)^\ell\rho^n, \quad i_{\ell,m,n}(0) = \delta_{z,\ell+n}\rho\binom{z}{\ell}(1-\rho)^\ell\rho^n, \quad w_{\ell,m,n}(0) = r_{\ell,m,n}(0) = 0. \quad \text{(3)}$$

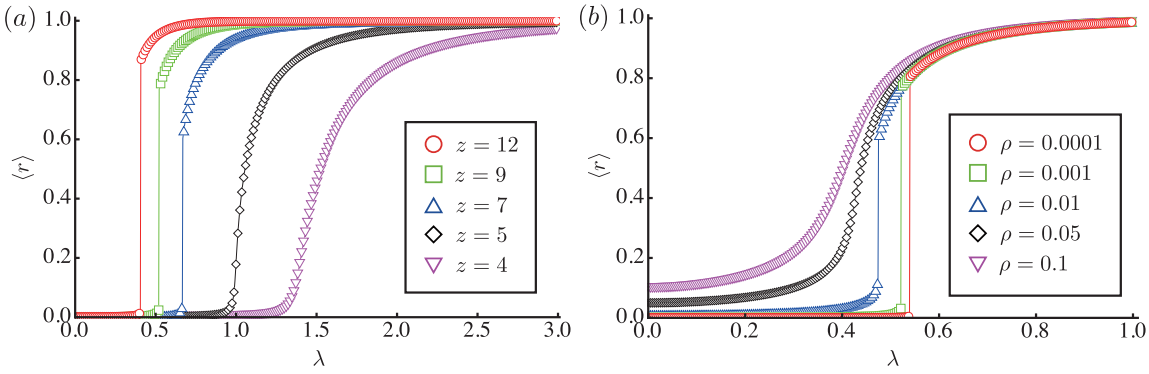

FIG. 4: (a) Mean final fraction of the removed nodes, $\langle r\rangle$, in the RRGs with $\rho = 0.001$ and $z = 12, 9, 7, 5$, and 4 (from the left to the right), and (b) mean final fraction of the removed nodes, $\langle r\rangle$, in the RRG with $z = 9$, and $\rho = 0.1, 0.05, 0.01, 0.001$, and 0.0001 (from the left to the right). The symbols and lines are obtained by evaluating the AMEs.

By evaluating the AMEs (1) with this initial condition, we obtain the total density of each state at time t as

$$s(t) = \sum_{\ell,m,n} s_{\ell,m,n}(t), \quad w(t) = \sum_{\ell,m,n} w_{\ell,m,n}(t), \quad i(t) = \sum_{\ell,m,n} i_{\ell,m,n}(t), \quad r(t) = \sum_{\ell,m,n} r_{\ell,m,n}(t). \tag{4}$$

In Fig. 3, we plot the fraction of R nodes, $\langle r\rangle$, in the final states using the AMEs and the Monte Carlo simulations. Here $\langle r\rangle = r(t \to \infty)$ for the AMEs. The AMEs clearly show that there is a discontinuous jump of $\langle r\rangle$ at $\lambda_d \approx 0.522$, where a jump of $\langle r_{\max}\rangle$ has already been observed numerically. Indeed, the Monte Carlo simulations support the solutions of the AMEs: data related to $\langle r\rangle(N)$ approaches the line drawn by the AMEs as N increases.

Utilizing the AMEs for the SWIR model in the RRG with given values of ρ and z, we obtain the final density of each state with high accuracy and a short computation time, considering the z-dependence and ρ-dependence of $\langle r\rangle$. In Fig. 4 (a), we plot $\langle r\rangle$ for the case of $\rho = 0.001$ when the degree of the RRG changes ($z = 12, 9, 7, 5$, and 4). For a fixed ρ, the discontinuity of $\langle r\rangle$ is clearer in networks with larger degrees. This discontinuity, however, becomes weak as z decreases and it disappears in RRGs with small degrees of z (i.e., $z \leq 5$). In Fig. 4 (b), we plot $\langle r\rangle$ for the case where $z = 9$ when the seed fraction changes ($\rho = 0.1, 0.05, 0.01, 0.0001$, and 0.0001). We find that there is a discontinuous jump of $\langle r\rangle$ when ρ is small; it becomes less prominent as ρ increases, however, and it is eventually hard to distinguish an explosive spreading from the percolation of R clusters. We observe that the phase transition of the SWIR model with multiple seeds consists of two components: a percolation of R clusters and an explosive spreading of infections. The latter, however, disappears when ρ is too large and/or z is too small.

IV. SUMMARY

In this paper, we studied the spreading behaviors of the SWIR model in the RRGs. As previous studies have shown, the SWIR model starting from a single infected node exhibits a discontinuous transition at a certain infection rate, but when starting from a finite fraction of infected seeds, the model shows three different regimes that depends on the infection rate: the local epidemic phase, $\lambda < \lambda_c$, where clusters of removed nodes remains finite; the low global epidemic phase, $\lambda_c < \lambda < \lambda_d$, where a giant cluster of removed nodes (i.e., a giant R cluster) exists but the total fraction of removed nodes remains small; and the high global epidemic phase, $\lambda > \lambda_d$, where a giant R cluster occupies a large part of the network. We showed numerically that the first transition at λ_c is continuous in the same manner as an ordinary percolation transition, and that the second transition at λ_d is discontinuous. We formulated AMEs for the present model in order to demonstrate that the phase transition critically depends on both the degree of the underlying network and the fraction of initial seeds: the discontinuous transition disappears when the degree is small or when the seed fraction is large.

We focused on a simple version of the original SWIR model ($\kappa = 0$, $\lambda_1 = \lambda_2 = \lambda$, and $\mu = 1$). However, the present results are expected to hold true for the SWIR model itself. In [26], we have studied a multi-stage independent cascade model, which corresponds to a discrete-time SWIR model of $\lambda_2 = \kappa + \lambda_1$, and observed the same behavior, i.e., a discontinuous change of the order parameter in a percolating region.

As already mentioned, the present model is also used as a propagation model for innovations and transient fads [22]. The seed fraction determining whether a transition is continuous or discontinuous may be an important issue for viral

marketing campaigns. If there are few initial adopters (seeds), a viral marketing campaign becomes an all-or-nothing venture, i.e., there is only either complete success or complete failure, up to the influence between individuals. The cost effectiveness of marketing is otherwise rather reasonable: increasing initial adopters, or making the information more attractive, is directly linked to the number of individuals who will adopt the information.

Infectious diseases with finite fractions of infected seeds have been studied less than cases where there are single seed or infinitesimally small seed fractions. We know of almost no other complex epidemic models with finite seed fractions. Among complex epidemic models with finite seed fractions, a prospective one is cooperative epidemics [45–49]; in these, the infection of one disease stimulates the spreading of others. It will be interesting to see exactly how, and if, numerous seeds could cause catastrophic co-infections.

Acknowledgements

This work was partially supported by Grant-in-Aid for Young Scientists (B) (No. 15K17716), Grant-in-Aid for Scientific Research (B) (No. 26310203 and No. 16H03939), and Grant-in-Aid for Scientific Research (C) (No. 16K05507) from the Japan Society for the Promotion of Science (JSPS), and by JST, ERATO, Kawarabayashi Large Graph Project.

[1] R. Albert and A.-L. Barabási, Reviews of Modern Physics **74**, 47 (2002).
[2] M. E. J. Newman, SIAM Review **45**, 167 (2003).
[3] A. Barrat, M. Barthélemy, and A. Vespignani, *Dynamical processes on complex networks* (Cambridge University Press, Cambridge, 2008).
[4] S. N. Dorogovtsev, A. V. Goltsev, and J. F. F. Mendes, Reviews of Modern Physics **80**, 1275 (2008).
[5] R. Pastor-Satorras and A. Vespignani, Physical Review Letters **86**, 3200 (2001).
[6] Y. Moreno, R. Pastor-Satorras, and A. Vespignani, The European Physical Journal B-Condensed Matter and Complex Systems **26**, 521 (2002).
[7] W. O. Kermack and A. G. McKendrick, Proceedings of the Royal Society of London A: Mathematical, Physical and Engineering Sciences **115**, 700 (1927).
[8] R. M. Anderson and R. M. May, *Infectious Diseases of Humans: Dynamics and Control* (Oxford University press, 1992).
[9] R. Pastor-Satorras, C. Castellano, P. Van Mieghem, and A. Vespignani, Reviews of Modern Physics **87**, 925 (2015).
[10] J. C. Miller, A. C. Slim, and E. M. Volz, Journal of the Royal Society Interface **9**, 890 (2012).
[11] J. P. Gleeson, Physical Review Letters **107**, 068701 (2011).
[12] J. Lindquist, J. Ma, P. Van den Driessche, and F. H. Willeboordse, Journal of Mathematical Biology **62**, 143 (2011).
[13] J. P. Gleeson, Physical Review X **3**, 021004 (2013).
[14] A. V. Goltsev, S. N. Dorogovtsev, J. Oliveira, and J. F. F. Mendes, Physical Review Letters **109**, 128702 (2012).
[15] G. Ódor, Physical Review E **90**, 032110 (2014).
[16] P. Moretti and M. A. Muñoz, Nature Communications **4** (2013).
[17] G. Ódor, R. Dickman, and G. Ódor, Scientific Reports **5** (2015).
[18] W. Cota, S. C. Ferreira, and G. Ódor, Physical review E **93**, 032322 (2016).
[19] C. Castellano, S. Fortunato, and V. Loreto, Reviews of Modern Physics **81**, 591 (2009).
[20] D. Centola, V. M. Eguíluz, and M. W. Macy, Physica A **374**, 449 (2007).
[21] D. Centola, Science **329**, 1194 (2010).
[22] P. L. Krapivsky, S. Redner, and D. Volovik, Journal of Statistical Mechanics: Theory and Experiment **2011**, P12003 (2011).
[23] M. Zheng, L. Lü, M. Zhao, Physical Review E **88**, 012818 (2013).
[24] E. Campbell and M. Salathé, Scientific Reports **3** (2013).
[25] S. Melnik, J. A. Ward, J. P. Gleeson, and M. A. Porter, Chaos: An Interdisciplinary Journal of Nonlinear Science **23**, 013124 (2013).
[26] T. Hasegawa and K. Nemoto, Journal of Statistical Mechanics: Theory and Experiment **2014**, P11024 (2014).
[27] W. Wang, M. Tang, H.-F. Zhang, and Y.-C. Lai, Physical Review E **92**, 012820 (2015).
[28] D. J. O'Sullivan, G. J. O'Keeffe, P. G. Fennell, and J. P. Gleeson, Frontiers in Physics **3**, 71 (2015).
[29] J. C. Miller, Journal of Complex Networks **4**, 201 (2016).
[30] W. Wang, M. Tang, P. Shu, and Z. Wang, New Journal of Physics **18**, 013029 (2016).
[31] G. Bizhani, M. Paczuski, and P. Grassberger, Physical Review E **86**, 011128 (2012).
[32] K. Chung, Y. Baek, D. Kim, M. Ha, and H. Jeong, Physical Review E **89**, 052811 (2014).
[33] K. Chung, Y. Baek, M. Ha, and H. Jeong, Physical Review E **93**, 052304 (2016).
[34] D. Lee, W. Choi, J. Kertész, and B. Kahng, arXiv preprint arXiv:1608.00776 (2016).
[35] W. Choi, D. Lee, and B. Kahng, arXiv preprint arXiv:1608.02323 (2016).

[36] J. C. Miller, PloS ONE **9**, e101421 (2014).
[37] Z.-L. Hu, J.-G. Liu, G.-Y. Yang, and Z.-M. Ren, EPL **106**, 18002 (2014).
[38] S. Ji, L. Lu, C. H. Yeung, and Y. Hu, arXiv preprint arXiv:1508.04294 (2015).
[39] T. Hasegawa and K. Nemoto, Physical Review E **93**, 032324 (2016).
[40] T. Tomé and R. M. Ziff, Physical Review E **82**, 051921 (2010).
[41] D. R. de Souza, T. Tomé, and R. M. Ziff, Journal of Statistical Mechanics: Theory and Experiment **2011**, P03006 (2011).
[42] D. Stauffer and A. Aharony, *Introduction to percolation theory* (Taylor and Francis, London, 1994).
[43] T. Hasegawa, T. Nogawa, and K. Nemoto, EPL **104**, 16006 (2013).
[44] T. Hasegawa, T. Nogawa, and K. Nemoto, arXiv preprint arXiv:1407.3454 (2014).
[45] L. Chen, F. Ghanbarnejad, W. Cai, and P. Grassberger, EPL **104**, 50001 (2013).
[46] W. Cai, L. Chen, F. Ghanbarnejad, and P. Grassberger, Nature Physics (2015).
[47] L. Hébert-Dufresne and B. M. Althouse, Proceedings of the National Academy of Sciences **112**, 10551 (2015).
[48] P. Grassberger, L. Chen, F. Ghanbarnejad, and W. Cai, Physical Review E **93**, 042316 (2016).
[49] N. Azimi-Tafreshi, Physical Review E **93**, 042303 (2016).